# Effect of Bending Rigidity and Interfacial Permeability on the Dynamical Behavior of Water-in-Water Emulsions

**Elke Scholten, Leonard M. C. Sagis, and Erik van der Linden***

*Food Physics Group, Department of Agrotechnology and Food Sciences, Wageningen University, Bomenweg 2, 6703 HD Wageningen, The Netherlands*

*Received: November 11, 2005; In Final Form: December 29, 2005*

Phase separation in aqueous biopolymer mixtures results in the formation of an interface, separating two aqueous bulk phases. The properties of that interface are key parameters to understand and predict phenomena, such as the phase-separation process and deformation of droplets in a flow field. In these processes, the structures and sizes of the morphologies depend on the balance between viscous and interfacial forces. Normally, one assumes that the interfacial tension is the only important parameter regarding the interfacial forces. However, we will show that in these water-in-water emulsions, bending rigidity and interfacial permeability also play an important role. Spinning drop experiments show that at long time scales the interface is permeable to both dissolved biopolymers and water. From droplet relaxation experiments, we could conclude that, for shorter time scales, water is the only ingredient that can diffuse through the interface. Due to this permeability, these methods cannot be used to calculate the interfacial tension accurately, without taking into account the permeability of the interface. Including the permeability, we give a full description for the relaxation time of deformed droplets. From this description, the interfacial tension and the permeability of the interface can be deduced simultaneously. We also incorporate the permeability and the bending rigidity into the description of the kinetics of phase separation. From this theoretical description, we predict four different regimes to occur in the phase-separation process depending on the size of the domains. For the scaling of the domain size with time, we find an exponent of $^1/_4$ for bending- and permeability-dominated coarsening, an exponent of $^1/_3$ for bending-dominated coarsening, an exponent of $^1/_2$ for interfacial tension- and permeability-dominated coarsening, and an exponent of 1 for interfacial tension-dominated coarsening. The crossover between the different regimes depends on two different critical radii, $R_c$, equal to $(2k/\gamma)^{1/2}$ and $R_\lambda$, equal to $\eta\lambda_{eff}$. Taking values for the interfacial properties, we find these critical radii to be larger than a micrometer, indicating that both bending rigidity and permeability are of importance during phase separation.

## 1. Introduction

Biopolymer mixtures are very common in daily life, since they are used by many industries, such as the food industry, pharmaceutical industry, and cosmetics industry for the manufacture of a variety of products.[1−4] The mixtures of these natural ingredients phase separate already at low concentrations, and this is used to create different morphologies and structures with specific properties. Although the interfacial tension and morphologies of these biopolymer systems are studied extensively,[5−15] a complete understanding of biopolymer interfaces is still not available. Little attention has been given to other interfacial properties, such as interfacial thickness, bending rigidity, and interfacial permeability and their role in the dynamics of biopolymer mixtures. For oil−water interfaces, the interfacial tension is of the order of 1 mN/m. Since the bending rigidity of these interfaces is only of the order of 1 $k_BT$, the bending contribution to the interfacial energy can be neglected. Water−water interfaces, on the other hand, have an interfacial tension of the order of 1 $\mu$N/m, which is much smaller than that for oil−water interfaces. Since the interfacial thickness is much larger for water−water interfaces, the bending rigidity of these interfaces is expected to be much larger. Because the interfacial tension is very low, these bending contributions cannot be neglected for the description of the interfacial energy. The ability to transfer ingredients through the interface is also different when comparing water−water interfaces with oil−water interfaces. For oil−water interfaces, the permeability is determined by the solubility of the ingredients in the different solvents. In the case of water−water interfaces, the only solvent is water and therefore the permeability of the interface is determined by the structure of the interfacial region (size, concentration of biopolymers). Thus, water−water interfaces differ from oil−water interfaces regarding interfacial properties, such as interfacial thickness, interfacial tension, bending rigidity, and permeability. These interfacial properties play a role in the formation of morphologies in food and pharmaceutical products. The size of the domains and the structure of the morphology (droplet or bicontinuous) determine the macroscopic properties of the systems. When one of the components is able to gel, one could "freeze" the system in a particular morphology with domains with a particular length scale in order to control the properties of a product. Knowledge of the kinetics of the phase separation is thus desirable in order to control and predict the properties of biopolymer mixtures and to gain more insight on the relationship between these properties and phenomena such as phase separation and deformation of droplets.

This paper is divided into two parts. In the first part, we will show that permeability indeed plays a role in the case of water−

* To whom correspondence should be addressed. E-mail: erik.vanderlinden@wur.nl.

10.1021/jp056528d CCC: $33.50 
Published on Web 01/28/2006

water interfaces. Using experimental results obtained from spinning drop and droplet relaxation experiments, we show that water as well as both biopolymers are able to transfer through the interface. Including this permeability, we give a description for the relaxation time of the deformed droplets. In the second part, we will address the combined effects of interfacial tension, bending rigidity, and interfacial permeability on the coarsening rate of bicontinuous structures during phase separation. Our theoretical results show that we can expect four different regimes in the coarsening of these systems, depending on which interfacial property is most important at a specific domain size. The results show that in immiscible biopolymer systems, both bending rigidity and interfacial permeability may have a significant effect on the dynamics of these systems.

## 2. Effect of Permeability on Interfacial Tension Measurements

Interfacial tension is an important parameter in the dynamics of multiphase systems. Therefore, this parameter has been investigated extensively and has been measured using different techniques.[5−7,15−18] Since demixed biopolymer systems have a very low interfacial tension, in the order of 1 $\mu$N/m, not all available methods to measure interfacial tension are applicable to these systems. The techniques commonly used for these systems often involve the deformation of droplets, either in a flow field or in a rotational field. The interfacial tension can be determined from the degree of deformation or the relaxation time after the cessation of the flow field.[19−24] Both the spinning drop and the droplet relaxation methods are techniques widely accepted as reliable methods for the measurement of interfacial tension. However, these techniques are valid only in the case where the interfaces are not permeable to any of the components in the system and in the case where effects of the bending rigidity are negligible. This is indeed the case for normal liquid−air or oil−water interfaces. However, interfaces of phase-separated biopolymer mixtures are different since both coexisting bulk phases are mainly composed of the same component: 90% of each phase consists of water. Water does not favor one phase or the other and could diffuse through the interface to the other bulk phase. These interfaces can be compared to membranes that are permeable to certain components. Since in both techniques an external force field is applied in order to achieve deformation of the dispersed droplets, the system is no longer in equilibrium and permeability starts playing a role.

To test the validity of both the spinning drop and the droplet relaxation methods, we have measured the interfacial tension of mixtures of fish gelatin and dextran, for which we varied the dextran concentration, while the gelatin concentration was fixed at the concentration in the critical point. Figure 1 shows the phase diagram, where the open circles refer to the overall compositions of the mixtures. The compositions of the coexisting phases are denoted by the squares. The concentration of gelatin and dextran in both phases is determined with the use of polarimetry after the mixtures were phase separated. A more detailed description can be found elsewhere.[25]

For samples 2−6, we inserted a droplet of the low-density gelatin-rich phase in a capillary filled with the high-density dextran-rich phase. The capillary was then placed in a spinning drop apparatus, the SVT20 from Dataphysics, Germany, and rotated around its horizontal axis at a speed of 1000 rpm. For sample 1, we were not able to see the droplet because of the very small optical contrast between the two phases. Using a camera with a zoom function, we followed the droplet in time

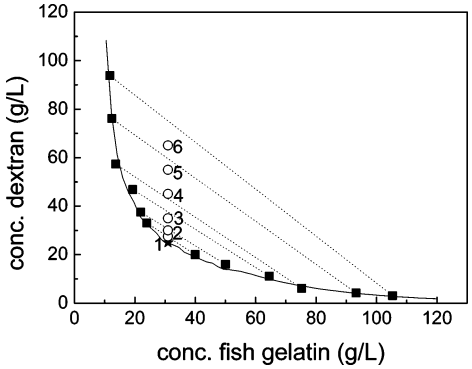


**Figure 1.** Phase diagram of the fish gelatin/dextran mixture. The open circles refer to the overall compositions, and the squares represent the composition of the coexisting phases. The square represents the critical point.

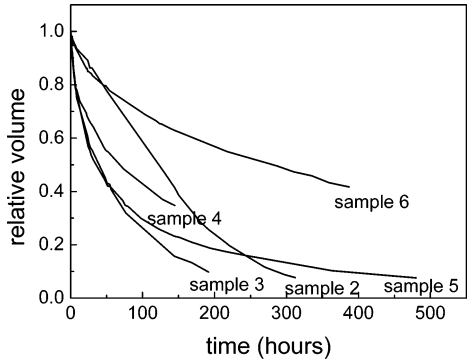


**Figure 2.** Changes in volume for different samples. The overall concentration and the concentration of the coexisting phases can be found in Figure 1, where they are represented as open circles.

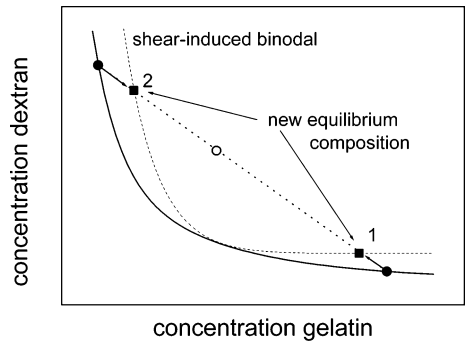


**Figure 3.** Schematic picture of the composition of the droplet in the capillary during the spinning drop experiment. The solid line refers to the binodal in rest. The dashed line refers to the shear-induced binodal (as provided by Puyvelde et al.[15]). The new equilibrium compositions of any overall composition (open circle) on the tie line (dotted line) are denoted by the squares. The old equilibrium compositions in rest are denoted by circles. The droplet phase is referred to as number 1 and the surrounding medium as number 2.

and observed that the volume of the dispersed droplets decreased in time. Over a period of a few days to weeks, the volume decreased up to 90% for most samples, as can be seen in Figure 2.

From these results, we could conclude that the interfaces are permeable to all components in the system. At the moment a force is applied (shear or rotation) on the system, the phase behavior is different than the phase behavior at rest and the binodal shifts as depicted in Figure 3.[15] The coexisting phases are therefore not in equilibrium with each other since the new equilibrium values will be on the new shear-induced binodal. The system will try to reach this new equilibrium state by

**TABLE 1: Diffusion Coefficients for the Three Components**

| sample | $D_1$ (m$^2$/s) | $D_2$ (m$^2$/s) | $D_3$ (m$^2$/s) |
|---|---|---|---|
| 2 | | | |
| 3 | $3.2 \times 10^{-12}$ | $3.2 \times 10^{-12}$ | $2.2 \times 10^{-13}$ |
| 4 | $3.9 \times 10^{-12}$ | $3.9 \times 10^{-12}$ | $2.2 \times 10^{-13}$ |
| 5 | $2.6 \times 10^{-12}$ | $3.9 \times 10^{-13}$ | $7.2 \times 10^{-14}$ |
| 6 | $1.3 \times 10^{-12}$ | $1.6 \times 10^{-14}$ | $1.6 \times 10^{-14}$ |

diffusion of components from one phase to the other. The outer phase will take up gelatin from the droplet in order to increase its gelatin concentration. However, since the volume of the surrounding medium is about 3 orders of magnitude larger than the volume of the droplet, the concentration will effectively stay the same, so the outer phase will never reach its new equilibrium composition. Therefore, the outer phase will continue to take gelatin from the droplet. To reach its new composition, the droplet will also expel water and dextran as a result of which the volume of the droplet decreases. The diffusion of all three components will continue until the droplet eventually disappears.

The diffusion process is considered to be Fickian, and we assume the total diffusion to be a linear addition of contributions from the diffusion of both the biopolymers and the water. With these assumptions, we can describe the total change in volume as[26]

$$V_{\text{total},t} = V_{\text{total},\infty} + \sum_i A_i \exp(-f_i t) \tag{1}$$

in which $i$ refers to the different components. The rate constant $f_i$ is related to a diffusion coefficient, $D_i$, and the diameter of the droplet, $d$, as[26]

$$f_i = \frac{4\pi^2 D_i}{d^2} \tag{2}$$

From this relation, we find three diffusion coefficients (Table 1) for which a clear identification in terms of the three components cannot be made, since the diffusion of the components is coupled. (For sample 2, we did not get satisfactory fits.)

The diffusion coefficients can be compared to the self-diffusion coefficients of the components, which can be estimated from the following relation

$$D_{\text{self}} = \frac{k_B T}{6\pi\eta R_h} \tag{3}$$

in which $k_B$ is the Boltzmann constant, $T$ is the temperature, $\eta$ is the viscosity, and $R_h$ is the hydrodynamic radius of the gelatin. For gelatin and dextran, we find self-diffusion coefficients of approximately $1 \times 10^{-12}$ m$^2$/s. Water has a self-diffusion coefficient of $2.3 \times 10^{-9}$ m$^2$/s, which is approximately 3 orders of magnitude larger than those of the biopolymers. Comparing the self-diffusion coefficients to the measured diffusion coefficients, we can conclude that the diffusion of the biopolymers determine the rate of the volume change.

Since all components are able to transfer through the interface, the properties of the bulk phase (concentration, density) and subsequently the properties of the interface (thickness, interfacial tension) will change in time. This makes the spinning drop method not suitable for the determination of the exact value for the interfacial tension. This method can be used only to obtain the right order of magnitude.

From the diffusion coefficients, we could conclude that the biopolymers determine the overall rate of the volume change. Since these biopolymers are relatively large, their self-diffusion coefficient is rather low, as a result of which the total diffusion process is rather slow; the decrease in volume of the dispersed droplet in the spinning drop experiments takes up to three weeks depending on their concentration. In the second technique (relaxation behavior) for the measurement of the interfacial tension, the time scale of the experiment is a few seconds only, which is much shorter than that in the case of the spinning drop experiments. One might expect that for these short time scales, the interfacial permeability is not important and that the relaxation behavior is dominated by the interfacial tension only. However, we will show that, although the time scales differ as much as 5 orders of magnitude, the interfacial permeability still plays a role.

In 1953, Oldroyd[27] already showed that for viscous liquids the characteristic relaxation time for the relaxation from an ellipsoidal shape to a spherical shape is given by

$$\tau = \frac{\eta R_0}{\gamma}\left[\frac{(19E+16)(2E+3)}{40(E+1)}\right] \tag{4}$$

in which $\eta$ is the viscosity of the continuous phase, $R_0$ is the size of the droplet after relaxation, $\gamma$ is the interfacial tension, and $E$ is the viscosity ratio of the dispersed and continuous phases. This indicates that when the relaxation time is plotted vs the droplet size, a straight line should be obtained that goes through the origin. From the slope of that line, the interfacial tension can be determined. However, our experiments (droplet relaxation after cessation of a flow field in a parallel plate shear cell, type CCS 450 from Linkam Scientific Instruments) show that when we fit our data with eq 4 these lines do not go through the origin, indicating that the interfacial permeability apparently does play a role in the process of relaxation. To give a full description of the relaxation of the droplet in time, the diffusion of the components has to be taken into account. Accounting for the interfacial tension and an effective permeability, $\lambda_{\text{eff}}$, of the interface, we find the following relation for the relaxation time of the droplet

$$\frac{1}{\tau} = \frac{40(E+1)}{(19E+16)(2E+3)}\frac{\gamma}{\eta R_0} + \frac{\lambda_{\text{eff}}\gamma}{{R_0}^2} \tag{5}$$

This description of the droplet relaxation indicates that, when the permeability is not taken into account, the interfacial tension is overestimated. Figure 4 shows the fits of eq 5 through the experimental data points. Table 2 shows the result of the determination of the interfacial tension with and without taking into account the permeability as an extra contribution to the relaxation time.

The permeability of samples close to the critical point (sample 1) is very high and decreases going further form the critical point. Therefore, the contribution of the permeability for samples close to the critical point is essential and has to be taken into account in order to determine the correct value for the interfacial tension. When this permeability is not taken into account, the interfacial tension can be overestimated by as much as 90%.

Figure 5 shows the permeability vs the interfacial tension. The data were fitted to the relation $\lambda_{\text{eff}} \sim \gamma^a$, for which the exponent $a = -0.9$ gave the best fit. Thus, the permeability seems to be inversely related to the interfacial tension $\lambda_{\text{eff}} \sim 1/\gamma$.

From scaling relations, we find that the permeability of these interfaces is related to an effective diffusion coefficient as $\lambda_{\text{eff}} \sim D_w/\gamma$. The diffusion coefficient was determined from the plot

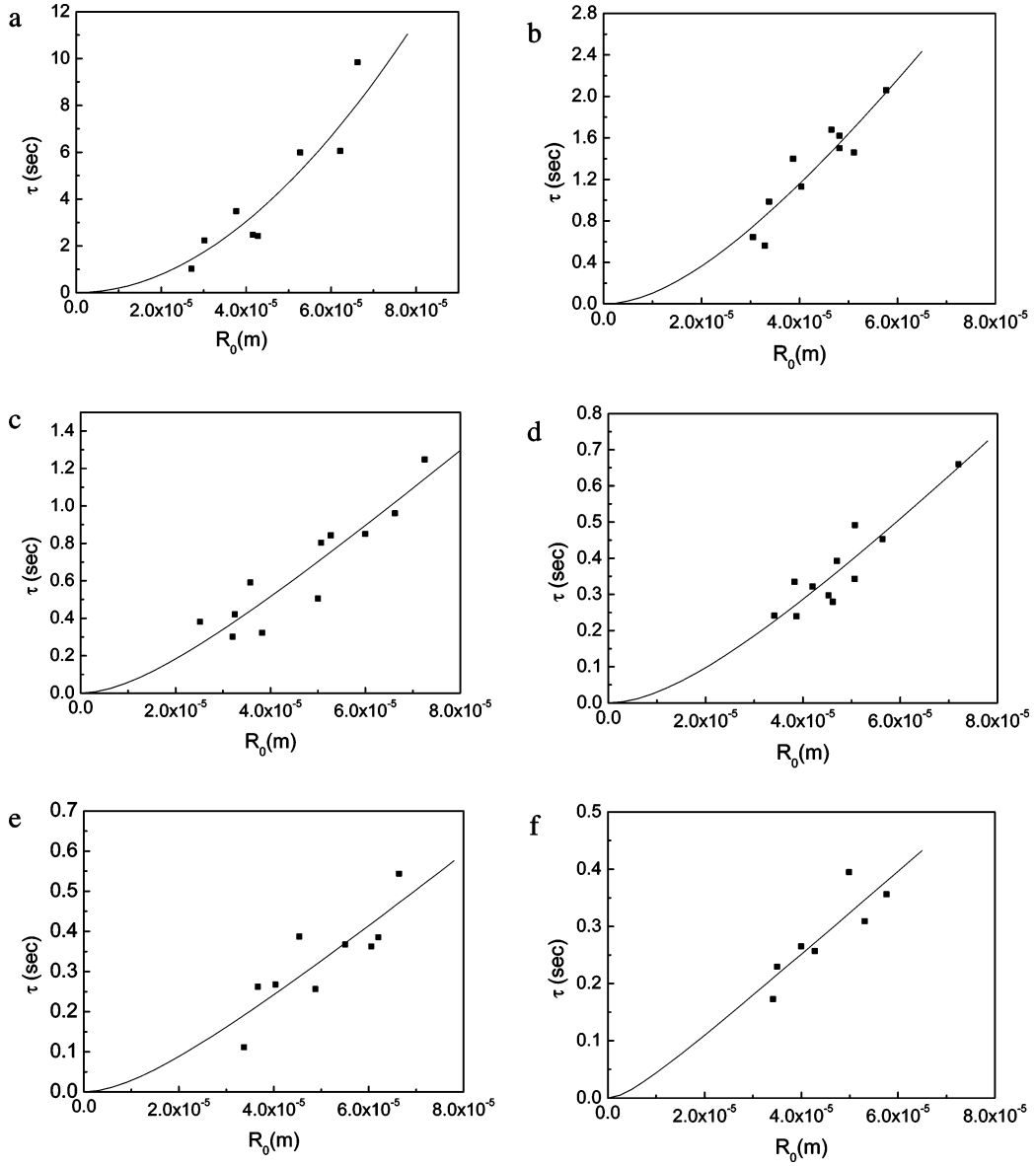


**Figure 4.** Characteristic relaxation time, $\tau$, plotted vs the deformed droplet, $R_0$: (a) sample 1, (b) sample 2, (c) sample 3, (d) sample 4, (e) sample 5, and (f) sample 6. The line is the best fit to eq 5, from which the interfacial tension and the permeability are calculated.

**TABLE 2: Interfacial Tension ($\lambda_1$) Calculated with Eq 5, the Interfacial Tension ($\lambda_2$) Calculated with Eq 4, and the Permeability, $\lambda_{eff}$, of Samples 1−6**

| sample | $\gamma_1$ ($\mu$N/m) | $\gamma_2$ ($\mu$N/m) | $\lambda_{eff}$ (m$^3$/N·s) |
|---|---|---|---|
| 1 | ≤0.01 | 0.15 | $\geq 5 \times 10^{-2}$ |
| 2 | 0.2 | 0.3 | $3.4 \times 10^{-3}$ |
| 3 | 1.0 | 1.2 | $1.3 \times 10^{-3}$ |
| 4 | 1.9 | 2.4 | $1.4 \times 10^{-3}$ |
| 5 | 4.6 | 5.1 | $5.3 \times 10^{-4}$ |
| 6 | 9.2 | 9.2 | $9 \times 10^{-5}$ |

of $\lambda_{eff}$ vs $1/\gamma$, and the slope of the fit through the data points was equal to $0.9 \times 10^{-9}$ m$^2$/s. This is comparable to the self-diffusion coefficient of water, $D_w^0$, which is equal to $2.3 \times 10^{-9}$ m$^2$/s. This indicates that water is the only component that diffuses through the interface. So, although the time scale in these experiments is rather short, the diffusion of the water molecules is still important in the relaxation behavior of the deformed droplets. The time sale is too short for the biopolymers to diffuse through the interface, since their self-diffusion coefficient is about 3 orders of magnitude smaller than that of water.

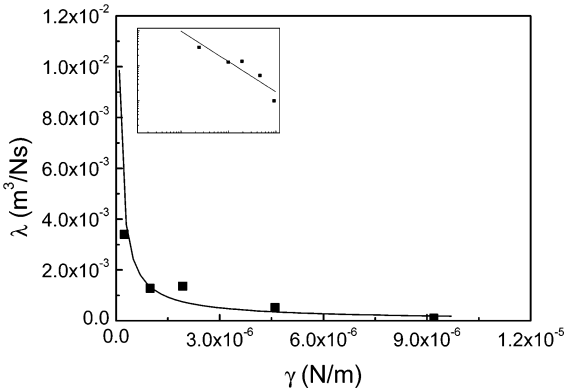


**Figure 5.** Permeability, $\lambda_{eff}$, plotted vs the interfacial tension, $\gamma$. The squares refer to the experimental data points. The solid line is the scaling relation $\lambda_{eff} \sim \gamma^{-0.9}$. The inset shows a double logarithmic plot.

Both the spinning drop and droplet relaxation method show that it is necessary to take the permeability of the interface into account for a full description of the behavior of an interface. As the time scale of the two methods differs by as much as 5

orders of magnitude, we see that different diffusion mechanisms play a role. During the relaxation of droplets, water is the only component that diffuses through the interface, while in the spinning drop method all components are exchanged from one phase to the other. Although the spinning drop method is too inaccurate to be able to measure the exact value for the interfacial tension, the droplet relaxation method can be used to measure the interfacial tension as long as the contribution of the permeability is taken into account. For samples far from the critical point only, the permeability of the interfaces is sufficiently small in order to ignore the contribution of the permeability term. Equation 4 would then be sufficient to determine the interfacial tension. For biopolymer systems, an alternative method for the determination of the interfacial tension would be a method that does not rely on the balance between the interfacial forces and another force field, which induces a pressure gradient. An example of such a method is described by Wijting et al.,[28] who determined the interfacial tension of a colloidal liquid−gas system using the meniscus of the interface at a fiber that is suspended in the system. The problem with this method is, however, that due to the low optical contrast and the very small sizes of the menisci, the contact is difficult to observe. They solved this problem by measuring dynamic contact angles by moving the fiber up and down. However, we do not know what the effect of this movement will be on the interface and to what extent the permeability of the interfaces would affect the results of such an experiment.

In this section, we have shown that permeability plays an important role in the case of water−water interfaces. As soon as a force field is applied on these systems, the transfer of biopolymers and water through the interface is possible. This indicates that when pressure gradients are present in the system, the permeability of the interface is of importance. One of the processes where pressure gradients are present is the phase-separation process. Since the shape and the size of the droplets change in time, pressure gradients across the interface are present and transfer through the interface is induced. In the next section, we will show the effect of this permeability and bending rigidity on the coarsening behavior of these systems.

### 3. Effect of Interfacial Permeability and Bending Rigidity on the Kinetics of Phase Separation

The kinetics of phase separation has received a lot of attention over the years, both experimentally and theoretically.[29−37] Although the mechanisms that have been proposed contribute to a better view of the phase-separation process,[38−47] a full understanding is still incomplete. In this section, we will show that for the coarsening of domains in bicontinuous structures due to hydrodynamic flow, the interfacial properties such as bending rigidity and interfacial permeability may also be of importance.

For bicontinuous structures, the coarsening rate is determined by the capillary instabilities of the domains. The interfacial energy induces a flow field in the domains, described by the Navier−Stokes equation

$$\rho \frac{\partial \vec{v}}{\partial t} + \rho(\vec{v}\cdot\nabla\vec{v}) = -\nabla\vec{P} + \rho g + \eta\nabla^2\vec{v} \qquad (6)$$

in which $\vec{v}$ is the flow velocity, $\rho$ is the density of the fluid, $P$ the thermodynamic pressure, $g$ the gravitational constant, and $\eta$ the viscosity of the fluid. For biopolymer mixtures in steady flow (i.e., $\partial\vec{v}/\partial t = 0$), the $(\vec{v}\cdot\nabla\vec{v})$ term and the gravitational term ($\rho g$) can be neglected, and eq 6 reduces to

$$0 = -\nabla\vec{P} + \eta\nabla^2\vec{v} \qquad (7)$$

Approximating the pressure gradient as $\Delta P/\Lambda$ and the Laplacian of the velocity by $\nu/\Lambda^2$, one arrives at

$$\eta\frac{\nu}{\Lambda^2} \approx \frac{\Delta P}{\Lambda} \qquad (8)$$

The difference in pressure ($\Delta P$) is determined by the interfacial tension, $\gamma$, and $\Lambda$ ($\Delta P \propto \gamma/\Lambda$). In general, the interfacial energy of the system is calculated using the interfacial tension of a flat interface, neglecting any curvature dependence of the interfacial energy. We take the curvature-dependent interfacial tension as described by Helfrich[48]

$$\gamma(\Lambda) = \gamma_0 + \frac{2k}{\Lambda^2} \qquad (9)$$

where $\gamma_0$ is the interfacial tension of the flat interface and $k$ is the bending rigidity. The first term signifies the stretching contribution to the interfacial energy, while the second term is related to the bending contribution. Combining eqs 8 and 9, we obtain

$$\frac{d\Lambda}{dt} \approx \frac{\gamma_0}{\eta} + \frac{2k}{\eta\Lambda^2} \qquad (10)$$

From the previous section, we have seen that the change in volume ($\sim d\Lambda^3/dt$) is determined not just by the interfacial tension but also by the permeability of the interface. From the differential mass balance, the volume change in time is related to the permeability and the pressure on the interface as $d\Lambda/dt \approx \lambda\Delta P$. Using the Laplace equation and eq 9, we find that as a result of mass transfer across the interface

$$\frac{d\Lambda}{dt} \approx \frac{\gamma_0\lambda_{\mathrm{eff}}}{\Lambda} + \frac{2k\lambda_{\mathrm{eff}}}{\Lambda^3} \qquad (11)$$

We assume that both mechanisms work in parallel. The coarsening of domains will be dominated either by interfacial tension driven flow in the bulk phases or by mass transfer across the interface depending on whether the interfacial tension or permeability is more relevant.

As all four terms have a different scaling with respect to domain size, the relative importance of these terms will change for different curvatures of the domains in the bicontinuous structures. As a result, we will observe different scaling behaviors as a function of domain size.

We can estimate the length scales for which the different interfacial properties become important and may become dominant in the phase-separation process. By equating both terms in eq 10 or 11, we find a critical, $R_c = (2k/\gamma)^{1/2}$, the critical radius below which the bending contribution dominates the stretching contribution to the interfacial energy. Equating the first terms of eqs 10 and 11, we find a critical radius, $R_\lambda \approx \lambda_{\mathrm{eff}}\eta$, the radius below which the phase-separation process will be more dominated by the permeability of the interfaces, rather than the interfacial tension. So, depending on the values for the different critical length scales, $R_c$ and $R_\lambda$, the scaling of the domain size with time for bicontinuous structures should show different regimes (in the limit of small and large length scales).

(i) A regime with a domain size larger than $R_c$ and $R_\lambda$ ($\Lambda \gg R_c$, $\Lambda \gg R_\lambda$). The coarsening process will then be dominated by the interfacial tension and eq 10 reduces to give

$$\frac{\Lambda_\eta}{\gamma} \propto t \tag{12a}$$

We see that in this regime, the domain size scales with time as $\Lambda \propto t$.

(ii) A regime with a domain size larger than $R_c$ but smaller than $R_\lambda$ ($\Lambda \gg R_c$, $\Lambda \ll R_\lambda$). The coarsening process will then be dominated by the interfacial tension and the permeability of the interface. The first term on the right side of eq 11 will be dominant and leads to the following relation with time

$$\frac{\Lambda^2}{\gamma\lambda_{eff}} \propto t \tag{12b}$$

For this regime, the domain size scales with time as $\Lambda \propto t^{1/2}$.

(iii) A regime with a domain size smaller than $R_c$ but larger than $R_\lambda$ ($\Lambda \ll R_c$, $\Lambda \gg R_\lambda$). For this regime, the coarsening process is dominated by the bending rigidity and eq 10 reduces to

$$\frac{\Lambda^3\eta}{2k} \propto t \tag{12c}$$

which gives a scaling relation $\Lambda \propto t^{1/3}$.

(iv) A regime with a domain size smaller than $R_c$ and $R_\lambda$ ($\Lambda \ll R_c$, $\Lambda \ll R_\lambda$), where the second term of the right side in eq 11 will be most dominant and one arrives at

$$\frac{\Lambda^4}{2k\lambda_{eff}} \propto t \tag{12d}$$

For this regime, we find that the domain size scales with time as $\Lambda \propto t^{1/4}$.

So, depending on the values of the critical sizes $R_c$ ($(2k/\gamma)^{1/2}$) and $R_\lambda$ ($\eta\lambda_{eff}$), we find scaling exponents ranging from $^1/_4$ to 1. We find an exponent of $^1/_4$ for bending- and permeability-dominated coarsening, an exponent of $^1/_3$ for bending-dominated coarsening, an exponent of $^1/_2$ for interfacial tension- and permeability-dominated coarsening, and an exponent of 1 for interfacial tension-dominated coarsening in bicontinuous structures. Scaling exponents ranging between $^1/_3$ and 1 have already been observed by Loren et al. for mixtures of gelatin and maltodextrin.[35]

We can estimate the length scales $R_c$ and $R_\lambda$ by taking into account the values for the separate interfacial properties. As we have seen in the previous section, the interfacial permeability of these interfaces is of the order of $1 \times 10^{-3}$ m$^3$/N·s. Taking a value for the viscosity of a viscous fluid as $10 \times 10^{-3}$ Pa·s, we find a critical radius $R_\lambda$ of approximately 10 $\mu$m. So, below length scales of 10 $\mu$m, the permeability of the interfaces will dominate the coarsening behavior. We can estimate the other critical radius $R_c$ from the values of the interfacial tension and the bending rigidity. From the previous section, we see that the interfacial tension is of the order of $1 \times 10^{-6}$ N/m. The bending rigidity of these interfaces is difficult to determine experimentally, since due to their low interfacial tension, they are very sensitive to small fluctuations in temperature, pressure, vibrations, etc.[49] Therefore, we have used a new model that calculates the bending rigidity with the use of the interaction potential between the biopolymers and the measured interfacial tension, as described elsewhere.[50] Table 3 shows the results of these calculations.

The results from these calculations show that the bending rigidity of these biopolymer interfaces are of the order of 500 $k_bT$, which is approximately an order of magnitude larger than values found for microemulsions and vesicles, which range from 1 $k_bT$[51] to 100 $k_bT$.[52] Since the interfacial tension is very low, the bending rigidity becomes relatively more important. Taking these values for the bending rigidity and realistic values for the interfacial tension, we find a critical radius of about 1 $\mu$m. Thus, for droplets smaller than a micrometer, bending contributions will dominate the stretching contribution to the interfacial energy.

**TABLE 3: Interfacial Tension, $\gamma$, and Bending Rigidity, $k$, for the Gelatin/Dextran System**

| interfacial tension ($\mu$N/m) | bending rigidity ($k_bT$) |
|---|---|
| 0.6 ± 0.1 | 763 ± 394 |
| 1.9 ± 0.3 | 985 ± 175 |
| 3.4 ± 0.3 | 665 ± 73 |
| 5.3 ± 0.4 | 714 ± 49 |
| 7.1 ± 0.4 | 566 ± 49 |
| 9.1 ± 0.6 | 615 ± 49 |

So, depending on the interfacial properties, the coarsening of the domains in bicontinuous structures will exhibit different scaling depending on the length scales in the system. As both critical length scales, $R_c$ and $R_\lambda$, have values that are of importance in the phase-separation process, the permeability and the bending rigidity of the interfaces have to be taken into account for a full description of the hydrodynamic flow. Depending on the critical length scales and the size of the domains, the different regimes for the coarsening rate can be expected.

These results show that, in the case of aqueous phase-separated biopolymer mixtures, the interfacial permeability and the bending rigidity cannot be ignored when discussing interfacial-related phenomena, such as phase separation, droplet morphologies, shear-induced phase separation, and droplet deformation. Normally, these interfacial properties are not taken into account, but as we have seen, they can have a large effect on these biopolymer mixtures. As the interfaces are permeable to all ingredients, pressure gradients that are exerted across the interface will induce the diffusion of both water and biopolymers. So, to be able to describe the interfacial phenomena under force fields, such as shear, this permeability has to be taken into account. The bending rigidity of the interfaces might be of importance as well. Since these bending rigidities are very high and interfacial tension is very low in these systems, this interfacial parameter has to be taken into account when dealing with large curvatures, for example, small droplet size. Especially for phenomena such as phase separation, the kinetics of the process will be influenced by all interfacial properties.

## Conclusion

In this paper, we have discussed the effect of interfacial properties, such as interfacial tension, interfacial permeability, and bending rigidity, on the dynamics of aqueous phase-separated biopolymer mixtures. From spinning drop experiments and the relaxation behavior of droplets after the cessation of a flow field, we have shown that the interfaces of these mixtures are permeable. Different ingredients will diffuse through the interface depending on the time frame of the experiment. In the spinning drop experiment, we see that the interface is permeable to all ingredients of the system and that the rate of the diffusion process is dominated by the diffusion of the biopolymers in the system. Since this permeability is not taken into account in the analysis of the spinning drop method, this method is not valid for the measurement of the exact value for the interfacial tension. In the relaxation experiments, we have

found the water to be the only ingredient to diffuse through the interface, since the time scale was much shorter. Taking into account this permeability, we give a new description for the relaxation process from which the interfacial tension and the permeability can be deduced simultaneously. Without taking into account this extra parameter, this method is not valid for the determination of the interfacial tension. We show that this permeability as well as the bending rigidity has an effect on the phase-separation process. We incorporate the permeability and the bending rigidity into the description of the hydrodynamic flow for bicontinuous structures. We find two critical length scales, $R_c$, equal to $(2k/\gamma)^{1/2}$, and $R_\lambda$, equal to $\eta\lambda_{eff}$. Depending on the value for these critical length scales, we find different regimes for the scaling of the domain size with time. For domain sizes larger than $R_c$ and $R_\lambda$ ($\Lambda \gg R_c$, $\Lambda \ll R_\lambda$), the coarsening is dominated by the interfacial tension only and the domain size scales with time as $\Lambda \propto t$. For domain sizes larger than $R_c$ but smaller than $R_\lambda$ ($\Lambda \gg R_c$, $\Lambda \ll R_\lambda$), we find an interfacial tension- and permeability-dominated coarsening for which the domain size scales with time as $\Lambda \propto t^{1/2}$. When the domain size is smaller than $R_c$ ($\Lambda \ll R_c$), the coarsening is dominated by the bending rigidity, rather than the interfacial tension. When the domain size is larger than $R_\lambda$ ($\Lambda \gg R_\lambda$), we find a scaling of $\Lambda \propto t^{1/3}$, and when the domain size is smaller than $R_\lambda$ ($\Lambda \ll R_\lambda$), the coarsening is also dominated by the permeability and we find the scaling relation $\Lambda \propto t^{1/4}$. Using a model, we calculate the bending rigidity in order to estimate the critical length scales. From these calculations, we see that the bending rigidities are very high for these systems, which gives a critical radius of $R_c$ of approximately 1 $\mu$m. Using values for the viscosity of these viscous fluids and the permeability of these systems, we find a critical radius $R_\lambda$ of approximately 10 $\mu$m. Both critical radii are of such extent that the interfacial permeability and the bending rigidity have to be taken into account in the description for the interfacial forces for interfacial-related phenomena.

## References and Notes


(1) Kasapis, S.; Morris, E. R.; Norton, I. T.; Gidley, M. J. *Carbohyd. Polym.* **1993**, *21*, 249−259.
(2) Kasapis, S.; Morris, E. R.; Norton, I. T.; Brown, C. R. T. *Carbohyd. Polym.* **1993**, *21*, 261−268.
(3) Goff, H. D. *Int. Dairy J.* **1997**, *7*, 363−373.
(4) Bot, A.; Mellema, M.; Reiffers-Magnani, C. K. *Ind. Proteins* **2003**, *11*, 11−13.
(5) Ding, P.; Wolf, B.; Frith, W. J.; Clark, A. H.; Norton, I. T.; Pacek, A. W. *J. Colloid Iinterface Sci.* **2002**, *253*, 367−376.
(6) Guido, S.; Simeone, M.; Alfani, A. *Carbohyd. Polym.* **2002**, *48*, 143−152.
(7) Lundell, C.; Walkenström, P.; Lorén, N.; Hermansson, A.-M. *Food Hydrocolloids* **2004**, *18*, 805−815.
(8) Guido, S.; Villone, M. *J. Rheol.* **1998**, *42*, 395−415.
(9) Doublier, J. L.; Garnier, C.; Renard, D.; Sanchez, C. *Curr. Opin. Colloid Interface Sci.* **2000**, *5*, 202−214.
(10) Edelman, M. W.; van der Linden, E.; de Hoog, E.; Tromp, H. *Biomacromolecules* **2001**, *2*, 1148−1154.
(11) Loren, N.; Hermansson, A. M. *Int. J. Biol. Macromol.* **2000**, *27*, 249−262.
(12) Bourriot, S.; Garnier, C.; Doublier, J. L. *Int. Dairy J.* **1999**, *9*, 353−357.
(13) Butler, M. F.; Heppenstall-Butler, M. *Biomacromolecules* **2001**, *2*, 812−823.
(14) Butler, M. F. *Biomacromolecules* **2002**, *3*, 1208−1216.
(15) van Puyvelde, P.; Antonov, Y. A.; Moldenaers, P. *Korea-Aust. Rheol. J.* **2002**, *14*, 115−119.
(16) Pacek, A. W.; Ding, P.; Nienow, A. W. *Chem. Eng. Sci.* **2001**, *56*, 3247−3255.
(17) Simeone, M.; Alfani, A.; Guido, S. *Food Hydrocolloids* **2004**, *18*, 463−470.
(18) van Puyvelde, P.; Antonov, Y. A.; Moldenaers, P. *Food Hydrocolloids* **2003**, *17*, 327−332.
(19) Vonnegut, N. *Rev. Sci. Instrum.* **1930**, *13*, 99.
(20) Princen, H. M.; Zia, I. Y. Z.; Mason, S. G. *J. Colloid Interface Sci.* **1967**, *23*, 99.
(21) Taylor, G. I. *Proc. R. Soc. A* **1932**, *138*, 41−48.
(22) Taylor, G. I. *Proc. R. Soc.* **1934**, *146*, 501−523.
(23) Lekkerkerker, H. N. W.; de Hoog, E. H. A. *Physica A* **2001**, *298*, 69−74.
(24) Mellema, J.; Blom, C.; Beekwilder, J. *Rheol. Acta* **1987**, *26*, 418−427.
(25) Scholten, E.; Visser, J. E.; Sagis, L. M. C.; van der Linden, E. *Langmuir* **2004**, *20*, 2292−2297.
(26) Berens, A. R.; Hopfenberg, H. B. *Polymer* **1978**, *19*, 489−496.
(27) Oldroyd, J. G. *Proc. R. Soc. London* **1953**, *218*, 122−132.
(28) Wijting, W. K.; Besseling, N. A. M.; Cohen-Stuart, M. A. *J. Phys. Chem. B* **2003**, *107*, 10565−10570.
(29) Anderson, V. J.; Jones, R. A. L. *Polymer* **2001**, *42*, 9601−9610.
(30) Butler, M. F.; Heppenstall-Butler, M. *Biomacromolecules* **2003**, *4*, 928−936.
(31) Verhaegh, N. A. M.; van Duijneveldt, J. S.; Dhont, J. K. G.; Lekkerkerker, H. N. W. *Physica A* **1996**, *230*, 409−436.
(32) Butler, M. F.; Heppenstall-Butler, M. *Food Hydrocolloids* **2003**, *17*, 815−830.
(33) de Hoog, E. H. A.; Tromp, R. H. *Colloids Surf., A* **2003**, *213*, 221−234.
(34) Williams, M. A. K.; Fabri, D.; Hubbard, C. D.; Lundin, L.; Foster, T. J.; Clark, A. H.; Norton, I. T.; Lorén, N.; Hermansson, A.-M. *Langmuir* **2001**, *17*, 3412−3418.
(35) Lorén, N.; Altskär, A.; Hermansson, A.-M. *Macromolecules* **2001**, *34*, 8117−8128.
(36) Siggia, E. D. *Phys. Rev. A* **1979**, *20*, 595−605.
(37) Dhont, J. K. G. *An introduction to dynamics of colloids*; Elsevier Science B. V.: Amsterdam, The Netherlands, 1996.
(38) Lifshitz, I. M.; Slyozov, V. V. *J. Phys. Chem. Solids* **1961**, *19*, 35−50.
(39) Binder, K.; Stauffer, D. *Phys. Rev. Lett.* **1974**, *33*, 1006−1009.
(40) Nikolayev, V. S.; Beysens, D.; Guenoun, P. *Phys. Rev. Lett.* **1996**, *76*, 3144−3147.
(41) Nikolayev, V. S.; Beysens, D. A. *Phys. Fluids* **1997**, *9*, 3227−3234.
(42) Tanaka, H. *Phys. Rev. Lett.* **1994**, *72*, 1702−1705.
(43) Tanaka, H. *J. Chem. Phys.* **1995**, *103*, 2361−2364.
(44) Cabral, J. T.; Higgins, J. S.; Yerina, N. A.; Magonov, S. N. *Macromolecules* **2002**, *35*, 1941−1950.
(45) Takeno, H.; Hashimoto, T. *J. Chem. Phys.* **1997**, *107*, 1634−1644.
(46) Crist, B. *Macromolecules* **1996**, *29*, 7276−7279.
(47) Chen, H.; Chakrabati, A. *J. Chem. Phys.* **1998**, *108*, 6006−6013.
(48) Helfrich, W. *Z. Naturforsch., C: J. Biosci.* **1973**, *28*, 693.
(49) de Hoog, E.; Lekkerkerker, H. N. W.; Schulz, J.; Findenegg, G. H. *J. Phys. Chem.* **1999**, *103*, 10657−10660.
(50) Scholten, E.; Sagis, L. M. C.; van der Linden, E. *J. Phys. Chem. B* **2004**, *108*, 12164−12169.
(51) Binks, B. P.; Meunier, J.; Abillon, O.; Langevin, D. *Langmuir* **1989**, *5*, 415−421.
(52) Bermudez, H.; Hammer, D. A.; Discher, D. E. *Langmuir* **2004**, *20*, 540−543.